Phase Separation Induced Morphology Evolution and Corresponding Impact Fracture Behavior of iPP/PEOc Blends

Yongyan Pang, Xia Dong, Ying Zhao, Charles C. Han, Dujin Wang

Beijing National Laboratory for Molecular Sciences, CAS Key Laboratory of Engineering Plastics and State Key Laboratory of Polymer Physics and Chemistry, Institute of Chemistry, Chinese Academy of Sciences, Beijing 100190, China

Received 12 September 2010; accepted 6 October 2010
DOI 10.1002/app.33686
Published online 22 February 2011 in Wiley Online Library (wileyonlinelibrary.com).

ABSTRACT: In this study, the influence of phase separation on impact toughness of isotactic polypropylene (iPP)/poly(ethylene-co-octene) (PEOc) blends was investigated. For the typical toughened polymeric system, three iPP/PEOc compositions (80/20, 70/30, and 60/40) were selected. When the polymeric blends were annealed at 200°C, the coarsening of phase domains was more prominent for the blend containing higher content of PEOc, and the scale of its morphological evolution was increased as well. The impact test showed that the impact strength variation trend as a function of annealing time was closely related to morphological evolution. It was believed that the sharpening of phase boundary and coarsening of phase domains were responsible for the depression of impact toughness, and the probable fracture mode alteration from shear banding to crazing and voiding. Structure evolution induced by phase separation showed an important effect on impact toughness, and it was also affected by the environmental conditions. Proper temperature was required to catch the tough-brittle transition induced by phase separation. © 2011 Wiley Periodicals, Inc. J Appl Polym Sci 121: 445–453, 2011

Key words: phase separation; morphology evolution; impact toughness; tough-brittle transition; isotactic polypropylene/poly(ethylene-*co*-octene) blend

INTRODUCTION

Because of poor impact toughness, especially under low temperatures, toughening of isotactic polypropylene (iPP) has been an interesting subject for several decades, from both industrial and scientific points of view. The modification of iPP ranges from the addition of rubbers,[1–5] thermoplastic elstomers,[6–13] rigid inorganic and organic fillers,[4,14] β-nucleating agent[15,16] to introduction of comonomers[17,18] and polymerization of in-reactor iPP catalloy,[19,20] etc. The well-known rubbery iPP modifiers included EPR, EPDM, SEBS, and so on.[1–5,21,22] In 1990s, the production of polyolefin elastomers became available, based on the copolymerization of ethylene and α-olefin, and since then, a new series of elastomeric species have been commercialized in vast amount. As a kind of rubbery thermoplastic, poly(ethylene-*co*-octene) (PEOc) exhibited easy processing characteristics, good dispersion in iPP matrix, and excellent toughness improvement of iPP/PEOc blends. These characteristics allowed the application of PEOc as a new iPP impact modifier, which had been proven to be an excellent substitute following the classical iPP modifiers.[6–13]

The famous toughening theories of rubber–polymer blends include crack termination at rubber particles, cavitation around rubber particles, matrix crazing, shear yielding, combined crazing and yielding, Wu's interparticle distance model and so on.[23–27] On the basis of kinds of traditional rubber toughened polymer systems, these toughening theories were established and developed from qualitatively to quantitatively. As referring to toughening effect, the term of brittle-tough transition was always used to describe the alteration of fracture modes from crazing to shear yielding.[21,28] According to the previous reports, the lower testing speed, higher temperatures, and higher content of rubber component were favored by shear yielding, while converse conditions were propitious for crazing formation.[21,28] The existence of structural defects such as notches, cracks, and bubbles could efficiently induce the formation of crazes.[21] Wu[25,26] proposed the definition of critical interparticle distance (ID_c), which was independent of rubber fractions and was the intrinsic characteristic of a given

Correspondence to: X. Dong (xiadong@iccas.ac.cn) and D. Wang (djwang@iccas.ac.cn).

Contract grant sponsor: National Natural Science Foundation of China; contract grant number: 50773087.

Contract grant sponsor: China National Funds for Distinguished Young Scientists; contract grant number: 50925313.

matrix. When the interparticle distance (ID) was smaller than the critical value (ID_c), the specimen manifested tough behavior; while conversely, the specimen would be fractured in a brittle manner. Wu also assumed that van der Waals attraction was strong enough for tough rupture; however, strong interfacial adhesion alone was not sufficient for toughening, and the value of ID must be smaller than that of ID_c.[25]

Although the toughening mechanisms and influencing factors of impact toughness of rubber-toughed polymers had been tremendously studied, the effect of phase separation on impact toughness had seldom been concerned.[21,23–26,28]. Up to date, the miscibility of polymer blends at molten state had been reported elsewhere,[12,29–31] but the miscibility of iPP/PEOc blends has seldom been reported. It was due to the closeness and crossover of refraction indices of the two components in a wide temperature range, and also due to the thermal degradation above 350°C. These became inevitable obstacles during experiments, and resultantly, a partially simulated phase diagram for iPP/PEOc blend system was established, instead of a complete one.[32,33] According to the phase diagram, iPP/PEOc blend manifests an upper critical solution temperature (UCST).[12,32–34] In a preceding report,[12] the time evolution of morphology and corresponding tensile properties of iPP/PEOc blends was investigated, and it was found that the sharpening of phase boundaries and decrease of interphase during the phase separation was responsible for the gradual breakage of tensile properties. In this study, the objective was mainly focused on the morphology evolution of iPP/PEOc blends induced by phase separation, and its effect on impact toughness and the corresponding fracture mechanisms.

EXPERIMENTAL

Materials and blending

Isotactic polypropylene (iPP1300) with $M_w = 4.1 \times 10^5$ and $M_w/M_n \sim 4$ was purchased from Beijing Yanshan PetroChemical Co. Poly(ethylene-*co*-octene) (PEOc, Engage 8150) with $M_w = 1.5 \times 10^5$, $M_w/M_n \sim 2$ and 30.6 wt % of 1-octene was provided by DuPont-Dow Elastomers. The molecular weight and molecular weight distribution were obtained from gel permeation chromatography (GPC). The content of octene was calculated according to the ^{13}C-NMR spectra.

The iPP/PEOc blend samples were named as PEOc-20, PEOc-30, and PEOc-40 containing 20, 30, and 40% weight percent of PEOc, respectively. The blends were prepared using a corotating twin screw extruder (TSE-30A) with an aspect ratio of L/D = 40. The temperatures were set as 180, 190, 200, 220, 220, 220, 220, 200, 190, and 180°C from feed zone to die zone, and the screw speed was 150 rpm. The blending was performed twice to achieve better dispersion.

Phase contrast optical microscopy

Phase contrast optical microscopy (PCOM) observations were carried out using a BX51 Olympus optical microscope connected with a Linkam THM S600 hot stage. The films with a thickness of $\sim$ 50 μm were prepared on a home-made compression molder. The samples were directly annealed at 200°C, identical with the sample preparation procedures for impact test. The phase contrast micrographs were taken during the annealing as the morphology evolved. The whole experimental procedures were under nitrogen protection.

Scanning electron microscopy

The morphologies of fractured surfaces of iPP/PEOc blends after the impact tests were investigated with a JSM-6700F JEOL scanning electron microscope (SEM) operated at 5 kV. The selected surface region was about 1.5 mm in distance to the V-notch. A deposition of a platinum layer on the fractured surface was performed prior to the observation.

Impact test

The pellets of PEOc-20, PEOc-30, and PEOc-40 were preheated at 200°C in a LP-*S*-50 compression molder for 5 min, then put on the pressure of 5 MPa for 2, 10, 30, 60, and 100 min respectively, at the same temperature, and then were quickly transferred to a TDM-50-2 compression molder to cool down, with temperature set at 35°C and pressure at 5 MPa.

The iPP/PEOc blend sheets prepared as described above were then cut out into rectangular bars with a RP/PCP pneumatic serving machine. The dimensions of rectangular impact bars were 64 mm × 10 mm × 4 mm. The V-notch was performed with a radius of 0.25 ± 0.05 mm on one edge of the impact bar, with equivalent distance to the two ends. Before impact test, three groups of specimens were kept for 48 h under three temperature conditions separately. The first group of specimens was put in an LRH-250A cultivation cabinet with constant temperature at 23°C, the second group was controlled at 0°C by ice water, and the third group was put into an LG 47NAD289 refrigerator at −20°C. Izod impact experiments were performed on an XJC-25D impact tester with an impact speed of 3.5 m/s. The vertical distance from the impact position to V-notch is 22 mm. The impact results presented were the average of eight specimens.

RESULTS AND DISCUSSION

The morphology evolution of iPP/PEOc blends was carried out via directly annealing the polymer

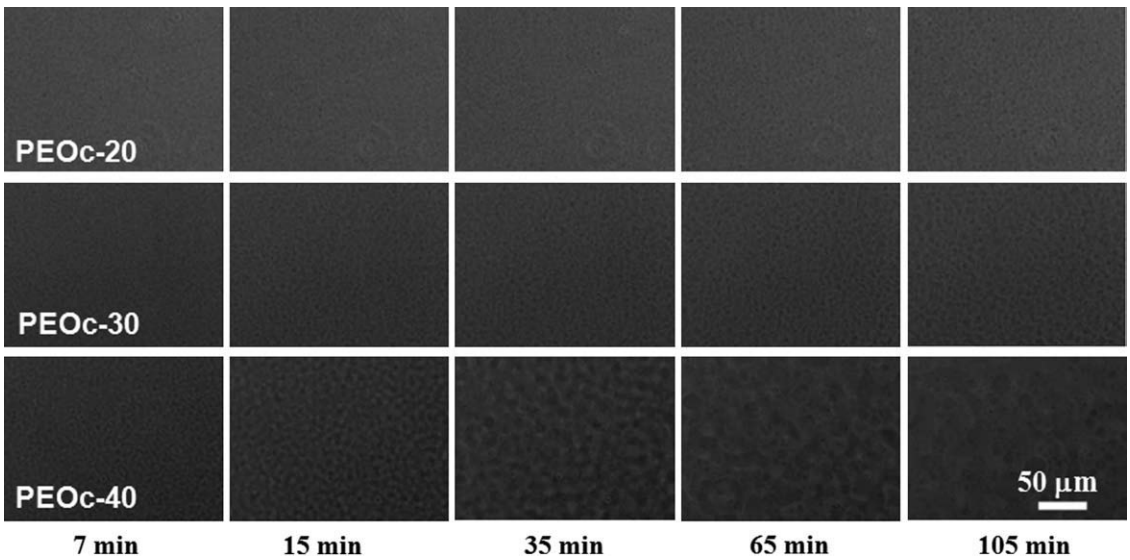

Figure 1 Phase contrast optical micrographs of PEOc-20, PEOc-30, and PEOc-40 annealing at 200°C for different time.

blends at 200°C, instead of quenching them from a homogeneous state to study the microstructure development. This was due to the aforesaid obstacles lying in experimental conditions and observations of iPP/PEOc blends.[12,32] On the basis of the partially stimulated phase diagram, PEOc-20, PEOc-30, and PEOc-40 were all in phase separation regions if annealed at 200°C. The morphology evolution of iPP/PEOc blends as a function of time was shown in Figure 1, displaying the phase domain coarsening during the annealing at 200°C. For all the three iPP/PEOc blends, the microstructure observation during annealing did not reveal complete circular liquid droplets growing, which implied that the phase separation mechanism was not nucleation and growth mechanism, but spinodal decomposition. It was consistent with the previous reports.[12] For samples of PEOc-20 and PEOc-30, after coarsening for a while, the bicontinuous interconnected structure was converted into separated island phase of the minority component dispersed in the sea phase. To examine closely, the bicontinuous interconnected structure was not very prominent for PEOc-20 even at the early stage (e.g., 7 min) during the annealing. It might be due to the off-critical and dissymmetrical composition of iPP and PEOc component. After a long time period of annealing (e.g. 105 min), the morphology of PEOc-40 still looked like the coexistence of bicontinuous and dispersed phase. Compared with the other two blends, PEOc-40 was closer to the critical composition. Resultantly, the bicontinuous interconnected structure of PEOc-40 could be maintained for a much longer period, and it might take more time to obtain the dispersed phase of the PEOc-rich domains. According to the previous studies, the mechanism of phase separation was fairly quick and complicated for the iPP/PEOc blends.[32,33] In addition, it has already emphasized that, due to the limited functions of compression molders, the iPP/PEOc blends were directly annealed at 200°C, instead of quenching from a homogenous state. As a result, the phase separation quickly went into a late stage of phase separation, thus the early stage of phase separation could not be caught and investigated; therefore the kinetics of phase separation was beyond the scope of this study. However, the increase of phase domain size was observed for all the three samples, and it was found closely related to the dissimilarity of the compositions of iPP/PEOc blends. The higher content of PEOc phase in this study, and the more prominently the phase domain size grew. Concomitant with the coarsening of phase domains, the phase boundary sharpened due to the concentration fluctuation. According to the concentration fluctuation model for two-component system established by Hashimoto et al.[29], at the late stage of SD, the two rich phase domains approaches the coexistence compositions, and the amount of interphase decreases during the coarsening.

The variation trend of Izod notched impact strength as a function of annealing time for PEOc-20, PEOc-30, and PEOc-40 was shown in Figure 2. The impact tests were carried out at 23, 0, and −20°C separately, and it was found that impact strength of the sample had strong dependence on the experimental conditions. When the impact test was conducted at 23°C, no obvious changes of impact strength values were observed for PEOc-20 specimen with the increase of annealing time, while brittleness dominated the failure in a brittle mode when the measurements were conducted at either 0 or −20°C [Fig. 2(a)], resulted from lower mobility of molecular

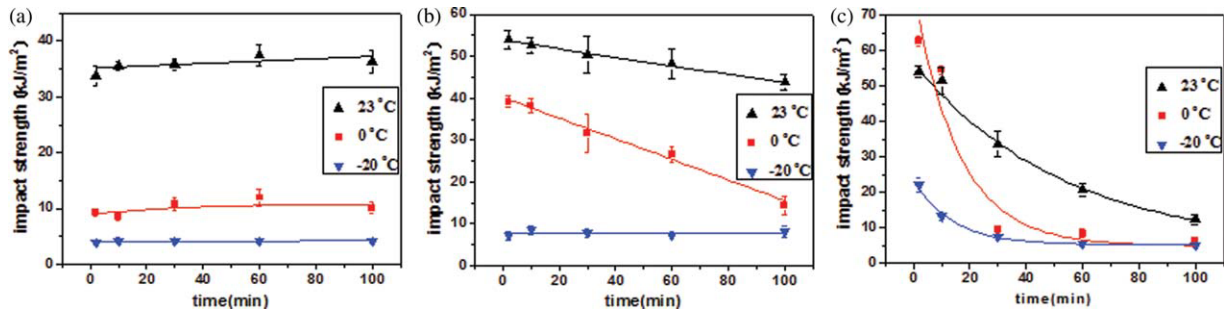

Figure 2 Izod notched impact strength as a function of annealing time at 200°C for samples: (a) PEOc-20, (b) PEOc-30, and (c) PEOc-40. The impact tests were conducted at 23, 0, and −20°C. [Color figure can be viewed in the online issue, which is available at wileyonlinelibrary.com.]

chains at lower temperatures. It also meant that the phase separation might almost be finished in a few minute when annealed at 200°C for sample PEOc-20, therefore the morphology did not change much and the corresponding impact properties was similar for specimens tested at the same temperature. As for PEOc-30 specimens impacted at 23 or 0°C, the values of impact strength display a linear depression with the annealing time. When the impact tests were conducted at −20°C, PEOc-30 samples were fractured in a brittle manner [Fig. 2(b)]. It indicated that the phase separation had some effect on the impact behavior of the sample with 30% PEOc component, which was consistent with the evolution of the morphology of PEOc-30 in Figure 1. By comparison, the value of impact strength of PEOc-30 [Fig. 2(b)] was found larger than that of PEOc-20 [Fig. 2(a)] annealed for the same period and tested at the same temperature, due to the higher content of elastomeric component and the better toughening effect. As for PEOc-40 specimens impacted at three temperatures, the impact strength values all display an exponential depression trend as a function of annealing time [Fig. 2(c)]. The impact strength was rapidly depressed to the lowest value for specimens annealed 30 min when they were impacted at −20°C, but annealed about 60 min when impacted at 0°C, and 100 min impacted at 23°C. It indicated that the phase separation has strong effect to the impact properties of the PEOc-40 samples. The longer the phase separation was conducted, the worse the impact strength was, and this trend was more prominent for specimens tested under lower temperature. And it was also observed that the lowest values of impact strength of PEOc-40 specimens tested at the three temperatures were about the same level as the lowest values of PEOc-20 and PEOc-30 samples. It meant that as long as the phase separation time was long enough, the toughening by the elastomer would be concealed, especially at lower temperatures. Compared the morphology evolution in Figure 1 and the impact strength variation in Figure 2, it was found that the depression of the impact strength showed the same iPP/PEOc composition dependence variation trend as the morphology evolution did. It was the most obvious for PEOc-40, the second was for PEOc-30, and the last one was for PEOc-20. The conclusion could be derived from the aforementioned results that, the depression trend of impact strength was closely related to the morphology changes of each specimen during the annealing, and that the depression of impact strength could also reflect the morphology evolution. It was mentioned here that when the impact tests were conducted at 23°C, the partial fracture of PEOc-40 specimens with short-term annealing manifested lower values than what they should be.

To essentially elucidate the mechanism of the influence of phase separation on impact toughness, the morphologies of fractured surfaces of impact specimens were investigated (Figs. 3–5) with SEM. Two kinds of morphologies were observed: one was the typically extensive shear bands, and the other was the rupture at the interphase between two phase domains, with semispherical holes and gibbosities visible on the fractured surfaces. According to the previous reports,[21,25,28,35] the fracture mechanism for the former type of morphology of the fractured surfaces was shear banding, while the latter one was crazing and voiding. The sample would manifest better toughness with fracture morphology of shear banding than crazing/voiding.

The PEOc-20 impact specimens (Fig. 3) conducted at 23°C were fractured in a tough manner with prominent shear bands on the fractured surface. An exception was the PEOc-20 specimen annealed at 200°C for 100 min, which showed the circular gibbosities of PEOc-rich domains on the fractured surface of the specimen. It indicated the coming tendency of fracture mode transition from shear banding to rupture at the interphase between iPP-rich and PEOc-rich domains with the increasing of phase separation time. When the impact tests were performed at 0 or −20°C, PEOc-20 specimens were fractured at the

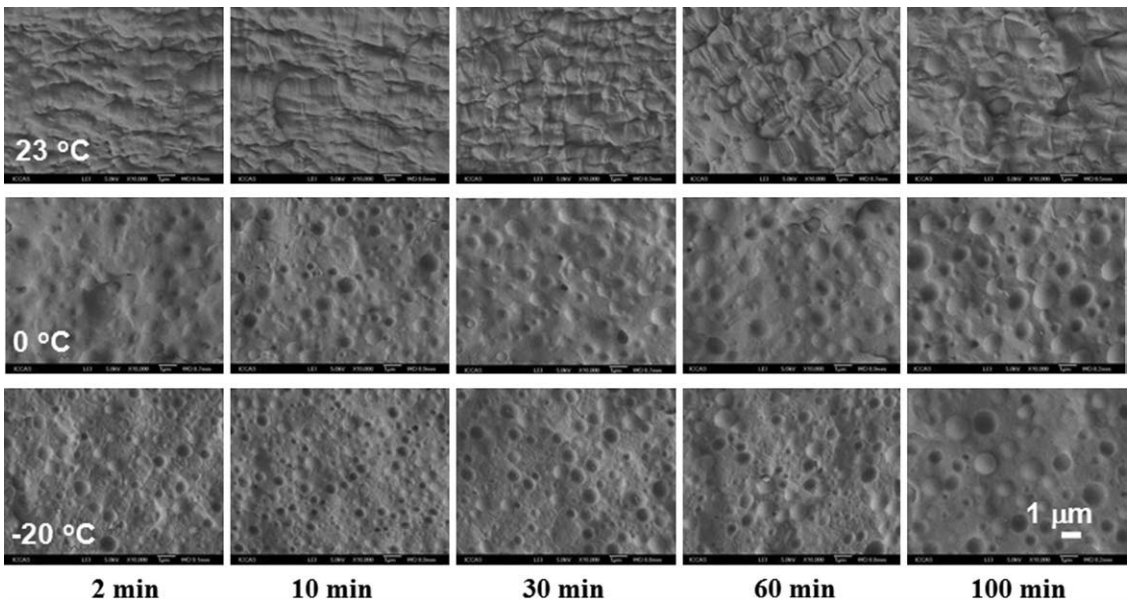

Figure 3 SEM images of fractured surfaces of PEOc-20 after annealing at 200°C for different time and then impacted at 23, 0, and −20°C.

interphase of iPP-rich and PEOc-rich domains, with hemispherical holes and gibbosities on the fractured surfaces. That's the typical morphology of a brittle failure. According to the previous reports, under applied external force, stress concentration was formed around the dispersed phase domains, and consequently, voiding, craze initiation, and crack propagation could happen at the interphase regions, resulting in delamination and separation of dispersed phase from the matrix.[25,35,36] As for PEOc-30 specimens tested at 23°C (Fig. 4), intensive shear banding was observed dominating the fracture mechanism. As the specimen was annealed for 100 min, the incoming tendency of the fracture manner alteration of PEOc-30 specimen also was observed. When PEOc-30 specimens were tested at −20°C, destructive breakdown at the phase boundaries dominated the fracture mode in a brittle manner. For measurements conducted at 0°C, it was found that the fracture mode was altered from shear banding to crazing and cavitation between the annealing time of 30 and 60 min. As it was discussed earlier, for all the samples

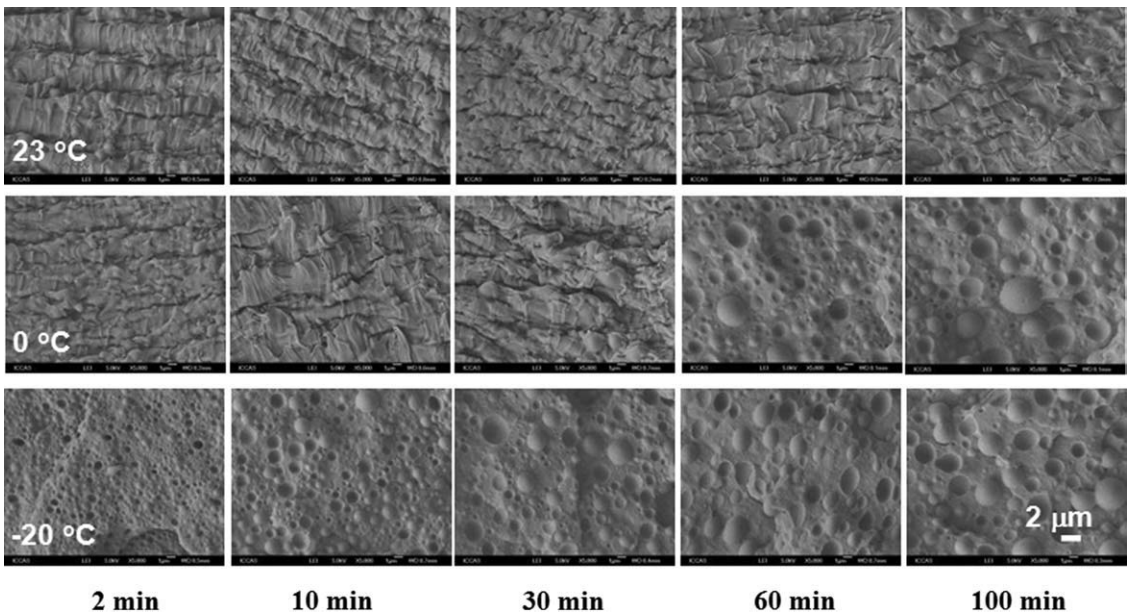

Figure 4 SEM images of fractured surfaces of PEOc-30 after annealing at 200°C for different time and then impacted at 23, 0, and −20°C.

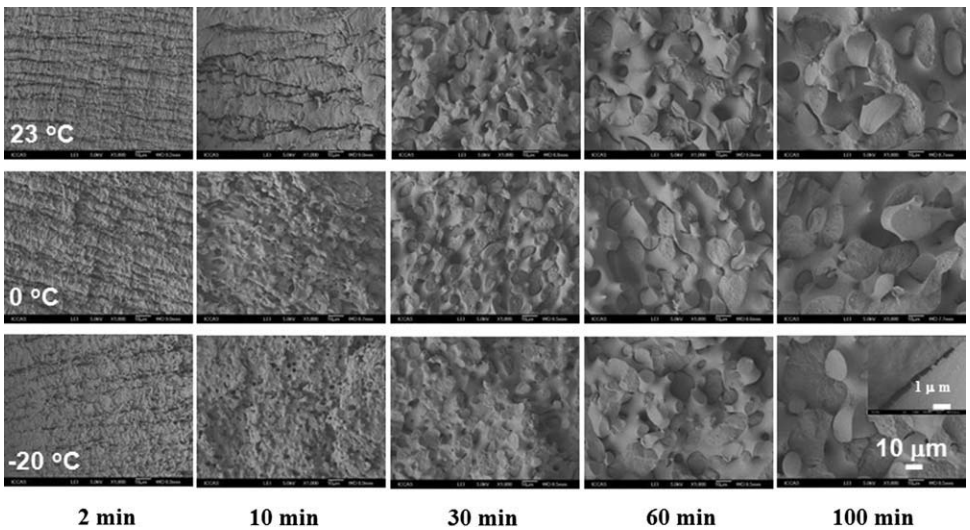

Figure 5 SEM images of fractured surfaces of PEOc-40 after annealing at 200°C for different time and then impacted at 23, 0, and −20°C. The inset is the localized magnification of interphase region.

annealing at 200°C, the coarsening of phase domains was the most obvious for PEOc-40 specimen. According to the phase diagram of this system,[33] the sample PEOc-40 was nearest to the critical point, therefore bicontinuous structure would be held for a long time and coarsening would be most prominent among the three samples. As a result, the fracture mode alteration from shear banding to crazing and voiding was fairly prominent for PEOc-40 specimens at all the three testing temperatures. Furthermore, the tough-brittle transition shifts to shorter annealing time direction as the testing temperature decreases (Fig. 5). In detail, the transition occurs between annealing time 10 and 30 min when PEOc-40 specimens were tested at 23°C, and around 10 min tested at 0°C, and between 2 min and 10 min tested at −20°C. It indicated that both lower temperature and longer phase separation time are favored by brittle failure. To catch the tough-brittle transition at a lower testing temperature, a shorter period of phase separation must be combined, otherwise, the specimen would probably be fractured in a brittle mode. Because of higher elastomer content in PEOc-40 blend than that in PEOc-20 and PEOc-30 blends, the PEOc-40 specimens undergoing a short-term phase separation could be able to manifest better impact toughness and still showed tough behavior tested even at −20°C. However, after a long-term annealing at 200°C, the size of phase domains of PEOc-40 exceeded 10 μm in diameter, and the boundaries of iPP and PEOc-rich domains were sharper and smoother. Voiding and crazing could probably be initiated at the sharper and smoother boundaries, which possess weak interfacial adhesion. These features were favored by crack propagation and exhaustive breakdown in a brittle manner. It was evidenced by the inset in Figure 5, which showed the weak interfacial adhesion for PEOc-40 annealed for a longer time, and easy separation of the two phase domains under external impact force. That's the origin for PEOc-40 specimens undergoing long-term annealing display brittle failure at 23°C, and its impact strength was even worse than that of PEOc-20 and PEOc-30 undergoing the same period of annealing.

One thing that needs to pay special attention was that the SEM morphologies of PEOc-20 and PEOc-30 specimens, especially impacted at low temperatures. These images showed that the sizes of PEOc-rich domains increased as the annealing time increased. All the dispersed phase domains were almost circular; while no bicontinuous interconnected morphology was observed. It seemed that the mechanism of phase separation for PEOc-20 and PEOc-30 specimens at 200°C was nucleation and growth. However, the crystallization had a significant effect on the phase separation and hence on the phase structure.[37] According to the previous reports,[38,39] the crystallization of iPP component could trap the PEOc-rich domains in iPP spherulites or push them in between the iPP crystals, and hence, iPP crystallization during cooling could affect the phase structure. Thus, the morphology shown by SEM was the structure captured at room temperature, which had already been affected by iPP crystallization during the cooling process, and it was not the real-phase structure at melt state during the annealing, as was shown by PCOM. Therefore, it is stated here that it is not proper to discuss the phase separation based on the morphology shown by SEM.

The testing temperature was an important factor for investigating the phase separation induced fracture mode transition. The tough-brittle transition for

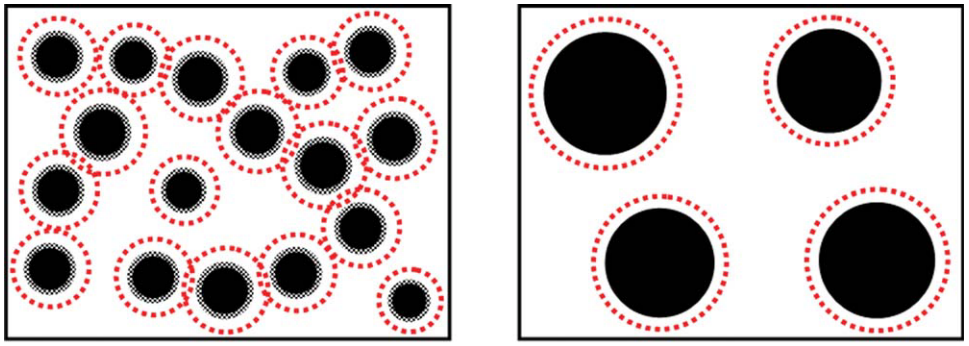

Figure 6 Schematic illustration of morphology evolution during annealing, changing from (a) smaller phase domains with diffuse boundaries to (b) larger phase domains with smoother boundaries. For simplification, the spherical domains of dispersed phase are employed instead of bicontinuous interconnected structure and irregular domains. The stress field surrounding the dispersed phase was enclosed by dashed circles. [Color figure can be viewed in the online issue, which is available at wileyonlinelibrary.com.]

PEOc-40 specimens was observed at all the three testing temperatures. The transition was observed at 0°C for PEOc-30, while it was not obtained for PEOc-20 at any of the three temperatures. However, it was deduced that the tough-brittle transition for PEOc-20 may be observed at the testing temperature between 0 and 23°C. Based on the dynamic mechanical thermal analysis, the glass transition temperatures of pure iPP and PEOc were at about 10 and −40°C, respectively. Accordingly, if the testing temperature was too much lower, the mobility of molecular chains was restricted to some extent, and the chains had less ability to respond to the applied external force, so that the specimens were more probably fractured in a brittle manner. As a result, all the PEOc-20 specimens were fractured in a brittle manner at 0 and −20°C, and all the PEOc-30 specimens manifested brittle failure at −20°C. However, the PEOc-40 specimens undergone short-term annealing still showed tough fracture behavior at −20°C, derived from higher elastomer content and less extent of morphology evolution. In comparison, if the testing temperature was too much higher, the specimens undergoing different periods of phase separation all would manifest tough behavior, and the influence of phase separation on impact fracture mechanism also would be covered up. Therefore, a proper testing temperature range was required in investigating the effect of morphology evolution on impact toughness. Tough-brittle transition controlled by phase separation might not be able to be observed if the specimens were tested at much higher or lower temperatures. In other words, impact toughness was strongly affected by the phase separation of the polymer blend, and also affected by environmental conditions.

It has been shown that the morphology evolution during phase separation of iPP/PEOc blends could alter the fracture mechanism from shear banding to crazing and voiding. The origin could be considered as follows. At the early stage of the annealing, the domain size was smaller and the interfacial adhesion at the phase boundaries is stronger. During the impact test, the elastomeric component could induce the yielding of the iPP matrix and results in extensive shear banding.[24,25] At the late stage of the annealing, the sizes of phase domains increased and the interphase sharpened due to the coarsening and concentration fluctuation. As a result, under the applied external impact force, the probable formation of voids and fibrils at the smoother phase boundaries around the larger phase domains might result in the catastrophic breakdown of the specimens. Therefore, the mechanism of voiding and crazing tended to dominate the fracture mode.[24,40–42] Note that the aforementioned discussion described the experiment that was conducted at a proper testing temperature.

The size of the rubber phase domain was a key factor characterizing the impact toughness of rubber–polymer blends. According to the previous reports,[25,42] more crazes could be induced around smaller rubber particles than larger ones, and larger impact strength would be obtained. To quantitatively characterize the impact toughness of rubber–polymer blends, Wu put forward the definition of interparticle distance (ID), namely, matrix ligament thickness. It was defined as the surface to surface distance of the two nearby particles and was determined only by the matrix, irrespective of the rubber species and fractions.[25,26] The ID could be determined from eq. (1):

$$\mathrm{ID} = d\left[\left(\frac{k\pi}{6V_r}\right)^{1/3} - 1\right] \tag{1}$$

where d was the rubber particle diameter, $k = 1$ for cubic packing, V_r was the rubber volume fraction.

For a certain polymer blend during annealing, V_r was constant. Estimating from eq. (1), as the coarsening proceeded, the phase domains grew in size, i.e., the values of d increased (see Figs. 1 and 3–5), and resultantly, ID increased. The increase of ID value usually gave rise to the depression of impact strength, especially when the value of ID was larger than that of ID_c.[2,25,26,36] The dispersed domains were always irregular in geometry, and thus precise calculation of the domain size and size distribution was considerably difficult in this study. Therefore, ID was taken as an explanation to qualitatively interpret the possible decrease of the impact strength of iPP/PEOc blends with longer period of annealing.

On the basis of the aforementioned experimental results and analysis, a schematic illustration was established to show the effect of phase separation on the impact strength, and on the probable fracture mode alteration (Fig. 6). The dark and white regions denoted the PEOc-rich and iPP-rich domains, respectively. For simplification, spherical domains of the dispersed phase were used, instead of bicontinuous interconnected morphology and irregular domains in geometry. At the relatively early stage of the annealing, the domain sizes and interparticle distances were smaller, and the sample posesses larger amount of interphase and higher interfacial adhesion. Once under the external impact, the stress field around the smaller dispersed domains would be joint or even overlapped with each other, and the specimens probably showed tough behavior, according to Wu's percolation model.[43,44] While at the late stage of the annealing, the domain sizes and interparticle distances were increased, and the sample possessed smoother phase boundaries and weaker connections. The stress field around the dispersed phase was weaker and independent on each other, resulting in the failure probably in a brittle mode, consistant with the reported studies.[4]

CONCLUSIONS

The influence of liquid–liquid phase separation on impact toughness of iPP/PEOc blends was investigated, which has seldom been reported. However, it was of great significance in guiding thermal treatment and processing from industrial points of view. On the basis of the foregoing results and analyses, some concluding remarks could be drawn as follows.

As the phase separation proceeded, the sizes of phase domains increased and the amount of interphase decreased, resulted from the concentration fluctuation and coarsening of phase domains. They were responsible for the gradual depression of impact toughness and the probable fracture modes alteration. Smaller dispersed domains and stronger interfacial adhesion were favored by the fracture mode of shear banding, while converse conditions were favored by crazing and voiding. An optimum testing temperature range was necessary to catch the shifting of deformation modes from shear banding to crazing and voiding.

References

1. van der Wal, A.; Gaymans, R. J Polymer 1999, 40, 6045.
2. Jiang, W.; Tjong, S. C.; Li, R. K. Y. Polymer 2000, 41, 3479.
3. Jiang, W.; Liu, C. H.; Wang, Z. G.; An, L. J.; Liang, H. J.; Jiang, B. Z.; Wang, X. H.; Zhang, H. X. Polymer 1998, 39, 3285.
4. Yang, H.; Zhang, X. Q.; Qu, C.; Li, B.; Zhang, L. J.; Zhang, Q.; Fu, Q. Polymer 2007, 48, 860.
5. Wang, Y.; Zhang, Q.; Na, B.; Du, R. N.; Fu, Q.; Shen, K. Z. Polymer 2003, 44, 4261.
6. McNally, T.; McShane, P.; Nally, G. M.; Murphy, W. R.; Cook, M.; Miller, A. Polymer 2002, 43, 3785.
7. Kontopoulou, M.; Wang, W.; Gopakumar, T. G.; Cheung, C. Polymer 2003, 44, 7495.
8. Da Silva, A. L. N.; Rocha, M. C. G.; Coutinho, F. M. B.; Bretas, R.; Scuracchio, C. J Appl Polym Sci 2000, 75, 692.
9. Da Silva, A. L. N.; Tavares, M. I. B.; Politano, D. P.; Coutinho, F. M. B.; Rocha, M. C. G. J Appl Polym Sci 1997 66, 2005.
10. Yang, J. H.; Zhang, Y.; Zhang, Y. X. Polymer 2003, 44, 5047.
11. Premphet, K.; Paecharoenchai, W. J Appl Polym Sci 2002, 85, 2412.
12. Pang, Y. Y.; Dong, X.; Zhao, Y.; Han, C. C.; Wang, D. J. Polymer 2007, 48, 6395.
13. Pang, Y. Y.; Dong, X.; Zhang, X. Q.; Liu, K. P.; Chen, E. Q.; Han, C. C.; Wang, D. J. Polymer 2008, 49, 2568.
14. Kurauchi, T.; Ohta, T. J Mater Sci 1984, 19, 1699.
15. Marco, C.; Gómez, M. A.; Ellis, G.; Arribas, J. M. J Appl Polym Sci 2002, 86, 531.
16. Li, X. J.; Hu, K. L.; Ji, M. R.; Huang, Y. L.; Zhou, G. E. J Appl Polym Sci 2002, 86, 633.
17. Fernando, P. L.; Williams, J. G. Polym Eng Sci 1981, 21, 1003.
18. Wang, L. X.; Huang, B. T. J Polym Sci Part B: Polym Phys 1990, 28, 937.
19. Greco, R.; Mancarella, C.; Martuscelli, E.; Ragosta, G.; Yin, J. H. Polymer 1987, 28, 1929.
20. Fu, Z. S.; Fan, Z. Q.; Zhang, Y. Q.; Feng, L. X. Eur Polym Mater 2003, 39, 795.
21. Jang, B. Z.; Uhlmann, D. R.; Vander Sande, J. B. J Appl Polym Sci 1984, 29, 3409.
22. Jang, B. Z.; Uhlmann, D. R.; Vander Sande, J. B. J Appl Polym Sci 1984, 29, 4377.
23. Maxwell, M. A.; Yee, A. F. Polym Eng Sci 1981, 21, 205.
24. Wu, S. H. J Polym Sci Part B: Polym Phys 1983, 21, 699.
25. Wu, S. H. Polymer 1985, 26, 1855.
26. Wu, S. H. J Appl Polym Sci 1988, 35, 549.
27. Yee, A. F. J Mater Sci 1977, 12, 757.
28. Matsushige, K.; Radcliffe, S. V.; Baer, E. J Appl Polym Sci 1976, 20, 1853.
29. Hashimoto, T.; Itakura, M.; Hasegawa, H. J Chem Phys 1986, 85, 6118.
30. Lohse, D. J Polym Eng Sci 1986, 26, 1500.
31. Ribbe, A. E.; Hashimoto, T. Macromolecules 1997, 30, 3999.
32. Yao, Y. H. Ph. D. Thesis, Institute of Chemistry, Chinese Academy of Sciences, 2006.
33. Yao, Y. H.; Dong, X.; Zhang, C. G.; Zou, F. S.; Han, C. C. Polymer 2010, 51, 3225.

34. Li, Z. W.; Lu, Z. Y.; Sun, Z. Y.; Li, Z. S.; An, L. J. J Phys Chem B 2007, 111, 5934.
35. Borggreve, R. J. M.; Gaymans, R. J.; Schuijer, J.; Ingen Housz, J. F. Polymer 1987, 28, 1489.
36. Jiang, W.; Liang, H. J.; Jiang, B. Z. Polymer 1998, 39, 4437.
37. Zhang, X. H.; Wang, Z. G.; Dong, X.; Wang, D. J.; Han, C. C. J Chem Phys 2006, 125, 024907–10.
38. Meng, K.; Dong, X.; Zhang, X. H.; Zhang, C. G.; Han, C. C. Macromol Rapid Commun 2006, 27, 1677.
39. Du, J.; Niu, H.; Dong, J. Y.; Dong, X.; Wang, D. J.; He, A. H.; Han, C. C. Macromolecules 2008, 41, 1421.
40. van der Wal, A.; Verheul, A. J. J.; Gaymans, R. J. Polymer 1999, 40, 6057.
41. van der Wal, A.; Gaymans, R. J. Polymer 1999, 40, 6067.
42. Dijkstra, K.; van der Wal, A.; Gaymans, R. J. J Mater Sci 1994, 29, 3489.
43. Margolina, A.; Wu, S. H. Polymer 1988, 29, 2170.
44. Gaymans, R. J.; Dijkstra, K. Polymer 1990, 31, 971.